J. Electrochem. Sci. Eng. **16** (2026) 3660; https://doi.org/10.5599/jese.3660

Open Access : : ISSN 1847-9286
https://pub.iapchem.org/ojs/index.php/JESE

Original scientific paper

Experimental investigation of electrochemical machining performance of AISI 304 stainless steel using a palladium-coated electrode with ascorbic acid - mixed electrolyte

Nethaji Subash Chandra Bose Ayyavoo[1], Saravanan Kandasamy Ganesan[1], Thirunavukkarasu Raja[2], Vinod Kumaar Jeevarathnam Ravi Kumar[3,✉], Lakshmanan Sankaralingam[4], Kumar Subramanian[5], Karthikeyan Saminathan[6] and Thangavel Thirugnanasambandham[7]

[1]*Department of Mechanical Engineering, Sona College of Technology, Salem 636007, India*
[2]*Department of Mechanical Engineering, SRM Institute of Science and Technology, Ramapuram campus, Chennai 600089, Tamil Nadu, India*
[3]*Department of Mechanical Engineering, Dr. N. G. P. Institute of Technology, Coimbatore, 641048, India*
[4]*Department of Aeronautical Engineering, Dayananda Sagar College of Engineering, Bangalore 560078, India*
[5]*Department of Production Engineering, Government College of Technology, Coimbatore 641013, India*
[6]*Department of Mechanical Engineering, Erode Sengunthar Engineering College, Palakarai 638057, Tamil Nadu, India*
[7]*Department of Mechanical Engineering, Saveetha School of Engineering, Saveetha Institute of Medical and Technical Sciences, SIMATS, Chennai 602105, Tamil Nadu, India*

Corresponding Author: ✉*jrvinod@gmail.com*

Received: August 30, 2026; Accepted: November 6, 2026; Published: November 14, 2026

Abstract

Passive film generation, buildup of insoluble hydroxide sludge, and dimensional errors caused by uncontrolled anodic dissolution are issues that arise during electrochemical machining (ECM) of AISI 304 stainless steel (SS). While electrode coatings and electrolyte additives have been studied separately, the combination of palladium (Pd)-coated electrodes and ascorbic acid-modified electrolytes to enhance ECM performance has received less attention. Using a Pd-coated needle electrode and a sodium nitrate ($NaNO_3$) electrolyte containing 10 g L^{-1} ascorbic acid, this study experimentally analyses the machining properties of AISI 304 SS. The effects on machining rate (MR) and overcut (OC) of electrolyte concentration (0.328 to 0.386 mol L^{-2}), machining voltage (7 to 12 V), duty cycle (40 to 90 %), and pulse frequency (40 to 90 Hz) were methodically assessed. The machined-hole shape was examined using scanning electron microscopy (SEM), and the

electrode substrate was characterized using energy-dispersive X-ray spectroscopy. Experimental data show that increasing electrolyte concentration, machining voltage, duty cycle, and pulse frequency enhanced MR and decreased OC within the examined ranges. With a 58.4 % improvement in MR from 0.219 to 0.347 µm s^{-1} and a 23.4 % decrease in OC from 290 to 222 µm when frequency increased from 40 to 90 Hz, pulse frequency showed the greatest increase in MR. At an electrolyte concentration of 0.386 mol L^{-1}, a machining voltage of 12 V, a 90 % duty cycle, and a pulse frequency of 90 Hz, the maximum recorded MR of 0.347 µm s^{-1} with an OC of 222 µm was attained. Nearly circular machined holes with comparatively clean edges and few surface deposits were visible in SEM examinations, suggesting regulated anodic dissolution. By reducing Fe^{3+} to Fe^{2+}, ascorbic acid is suggested to prevent the formation of insoluble ferric hydroxide, promoting electrolyte stability and eliminating reaction products. Using a Pd-coated electrode and an electrolyte modified with ascorbic acid, the study determines an experimentally assessed processing window for ECM of AISI 304 stainless steel, offering insights into increasing machining productivity and dimensional correctness.

Keywords
Electrochemical metal manufacturing; electrolyte composition; machining voltage; duty cycle; pulse frequency; machining rate; overcut

Introduction

Electrochemical machining (ECM) is a non-traditional manufacturing technique widely used to manufacture electrically conductive, difficult-to-machine materials such as titanium alloys, nickel-based superalloys, and stainless steels. To reduce tool wear, residual tensions, and heat damage, the technique entails controlled anodic dissolution of the workpiece without direct mechanical contact between the tool electrode and workpiece. Nevertheless, achieving high dimensional precision in ECM of AISI 304 stainless steel (SS) remains difficult. Unintentional material removal outside the planned machining zone due to stray-current-induced disintegration can cause overcut and inadequate dimensional control. Furthermore, the accumulation of electrochemical reaction products and the development of a passive oxide coating might impede homogeneous anodic dissolution and negatively impact surface quality and machining stability. The combined effects of process settings, electrolyte composition, and tool-electrode properties determine machining performance. A key strategy for enhancing current distribution, electrochemical stability, and dimensional precision during ECM is electrode surface modification.

Conductive and insulating coatings have been shown to be useful in enhancing machining performance in earlier studies. Yehia *et al.* [1] found enhanced electrical conductivity in Cu–WC composite coatings supplemented with graphene. To improve the surface quality of AISI 304 stainless steel by about 30 %, Kong *et al*. [2] devised a bipolar electrophoretic sidewall-insulation process for micro-hole machining. Similarly, Hung *et al.* [3] used microarc oxidation and hot-dip aluminizing to create insulating electrode coatings that enhanced drilling accuracy and decreased stray-current effects. While Hung *et al*. [4] showed improved hole geometry utilizing ceramic and epoxy coatings, Swain *et al*. [5] investigated nickel-coated tungsten microtools. Additional research by Hung and Chen [6] and Liu *et al.* [7,8] showed the efficiency of protective coatings and electrode insulation in reducing undesired dissolution and enhancing machining localization. All these studies show that altering the electrode surface is important for increasing ECM accuracy. However, there has been relatively little research done on the use of corrosion-resistant conductive coatings, especially palladium (Pd), for the ECM of AISI 304 SS.

(cc) BY

Another key method for enhancing anodic dissolution, electrolyte stability, and reaction product removal is altering the electrolyte. The ionic conductivity needed for ECM is provided by conventional sodium nitrate ($NaNO_3$) electrolytes; machining stability and dimensional precision may be impacted by the buildup of insoluble metallic hydroxides and the development of passive surface layers. As a result, researchers have investigated electrolyte additives, such as reducing and complexing agents, to enhance machining performance. For micro-hole machining of AISI 304 SS, Guodong *et al.* [9] examined a sodium citrate-modified $NaNO_3$ electrolyte and found that the material removal rate improved by about 35 %. The impact of complexing agent-assisted electrolytes on radial overcut (OC) during Ti6Al4V micro-drilling was investigated by Tak *et al.* [10]. When comparing a $NaNO_3$ - citric acid electrolyte system to a normal acidic electrolyte, Sethi *et al.* [11] found better surface properties and material solubility.

According to these investigations, appropriate electrolyte additions can affect dimensional accuracy, machining efficiency, and reaction-product buildup. Because of its reducing qualities, ascorbic acid ($C_6H_8O_6$) stands out among the available additions. To lessen sludge formation during electrochemical processing, Cercal *et al.* [12] investigated the effect of $C_6H_8O_6$ and ethylenediamine-tetraacetic acid (EDTA). According to their observations, $C_6H_8O_6$ reduced sludge-bulk by around 90 % in acidic settings (pH <5), while EDTA reduced it by about 30 % in alkaline conditions (pH >10). By reducing ferric ions (Fe^{3+}) to ferrous ions (Fe^{2+}), $C_6H_8O_6$ may minimize the precipitation of ferric hydroxide and enhance clearance of reaction products from the inter-electrode gap. These features imply that electrolytes treated with $C_6H_8O_6$ might have benefits for preserving steady ECM conditions. While electrode surface modifications and electrolyte additions have been studied separately, little research has examined the combined use of palladium-coated electrodes and $C_6H_8O_6$-modified $NaNO_3$ electrolytes for precision ECM of AISI 304 SS.

More research is needed to determine how electrolyte concentration, machining voltage, duty cycle, and pulse frequency affect machining rate (MR) and dimensional accuracy under this electrode-electrolyte setup. Finding operating settings that minimize lateral material removal while promoting controlled anodic dissolution requires an understanding of these interactions. Thus, using a palladium-coated needle electrode and a $NaNO_3$ electrolyte containing 10 g L^{-1} $C_6H_8O_6$, this work experimentally examines the ECM performance of AISI 304 SS. MR and OC are used to assess the impacts of electrolyte content (0.328 to 0.386 mol L^{-1}), machining voltage (7 to 12 V), duty cycle (40 to 90 %), and pulse frequency (40 to 90 Hz). Scanning electron microscopy (SEM) is used to describe the morphology of machined holes, and energy-dispersive X-ray spectroscopy (EDS) is used to investigate the composition of the tool electrode. The goals of the inquiry are to identify ideal machining conditions and elucidate the relationships between process parameters, material removal, and dimensional accuracy. The experimental assessment of this coupled electrode-electrolyte configuration and the identification of process conditions linked to enhanced machining performance within the examined parameter ranges constitute the main contributions of this work. When $C_6H_8O_6$ is added to the $NaNO_3$ electrolyte, this mechanism explains the observed rise in MR and decrease in OC [13-15].

In the present system, the following (electro) chemical reactions would be operative, Equations (1) to (9):

- dissociation of $NaNO_3$:
  $NaNO_3 \rightarrow Na^+ + NaNO_3^-$ (1)
- dissociation of ascorbic acid:
  $C_6H_8O_6 \leftrightarrow C_6H_7O^-_6 + H^+$ (2)

- anode reactions:
  $Fe \rightarrow Fe^{2+} + 2e^-$ (3)
  $Fe \rightarrow Fe^{3+} + 3e^-$ (4)
  $Cr \rightarrow Cr^{3+} + 3e^-$ (5)
  $Ni \rightarrow Ni^{2+} + 2e^-$ (6)
- reduction of ferric ions by ascorbic acid:
  $2Fe^{3+} + C_6H_8O_6 \rightarrow 2Fe^{2+} + C_6H_6O_6 + 2H^+$ (7)

where $C_6\ H_6\ O_6$ is dehydroascorbic acid (oxidized form).

Equation (7) suppresses the accumulation of Fe^{3+}, which would otherwise form insoluble sludges according to the Equation (8):

$Fe^{3+} + 3OH^- \rightarrow Fe(OH)_3\downarrow$ (8)

- cathode reaction:
  $2H_2O + 2e^- \rightarrow H_2\uparrow + 2OH^-$ (9)

Experimental

Machining voltage, duty cycle, electrolyte concentration, and frequency are process parameters that control ECM performance and are considered input factors. These parameters were chosen based on their effects on surface integrity, dimensional accuracy, MR, machining stability, and electrochemical dissolution. To find a stable machining window while avoiding unfavourable effects including arcing, excessive heating, passivation, and stray-current machining, preliminary experiments and available literature were taken into consideration. The stitching needle was used as a 500 μm diameter tool electrode, and a 0.5 mm-thick 304 SS workpiece was used for the study. The ECM process's accuracy, stability, and efficiency are all greatly influenced by the choice of machine parameters. The machining voltage (7 to 12 V), duty cycle (40 to 90 %), and electrolyte concentration (0.328 to 0.386 M $NaNO_3$ $C_6H_8O_6$ solution) used in this investigation were chosen based on available literature and electrochemical principles [16,17]. The chosen ranges were designed to minimize passivation, stray-current machining, excessive gas evolution, and heat impacts while offering stable electrochemical dissolution. In the present investigation, the machining time was recorded using a stopwatch. The MR was calculated by dividing the workpiece thickness (500 μm) by the machining time expressed in seconds. The overcut was determined from the difference between the machined-hole diameter, measured using optical images, and the nominal tool electrode diameter (500 μm).

Palladium is applied to the needle through sputtering. To remove any tiny particles that might have gathered on the electrode surface, the electrode was first immersed in isopropyl alcohol, double-distilled water, and ultrasonicated acetone. This clean electrode was placed inside the ultrahigh vacuum chamber. The UHV DC magnetron sputtering power was fixed at 30 W, the argon gas flow was maintained at 0.12 $m^3\ s^{-1}$, the base pressure was 40 μPa, and the deposition pressure was 0.53 Pa. With a 10 cm distance between it and the target, the electrode was pre-sputtered for 10 minutes while rotating at 10 rpm [18,19]. For a day, the prepared coated electrode is kept in a base vacuum (high vacuum). Figure 1 displays the profile of the tool electrode plated with palladium.

The EDS spectra of the palladium-coated needle used as the tool electrode in the electrochemical machining tests are displayed in Figure 2. Characteristic Ni peaks between 7.47 and 8.26 keV dominate the spectra, suggesting that the underlying needle substrate is mostly Ni-containing. Minor peaks also correlate with Fe, Si, Al, O and C. The presence of the palladium coating on the needle surface is confirmed by weak features in the 2.8 to 3.0 keV range, which can be attributed to Pd L-series emissions.

(cc) BY

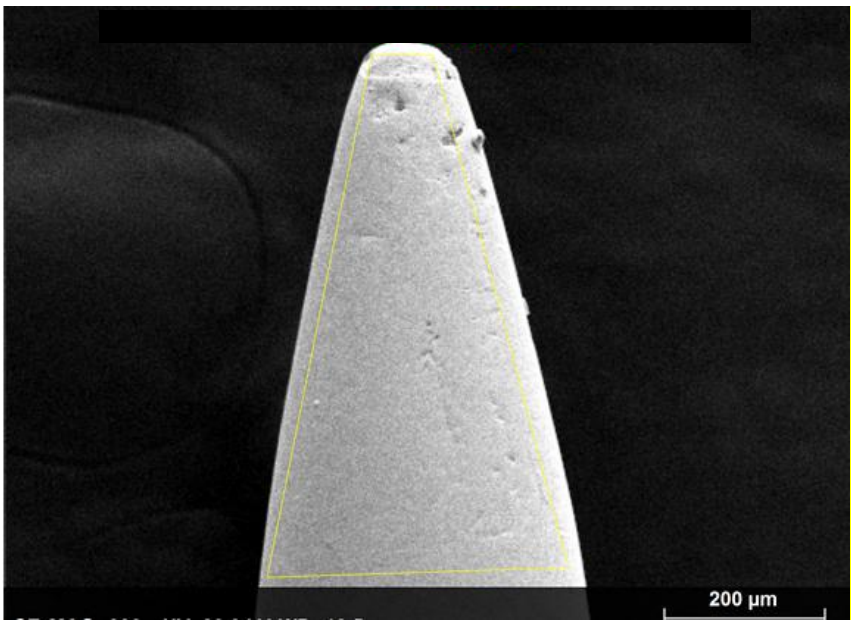


Figure 1. *Palladium coated electrode*

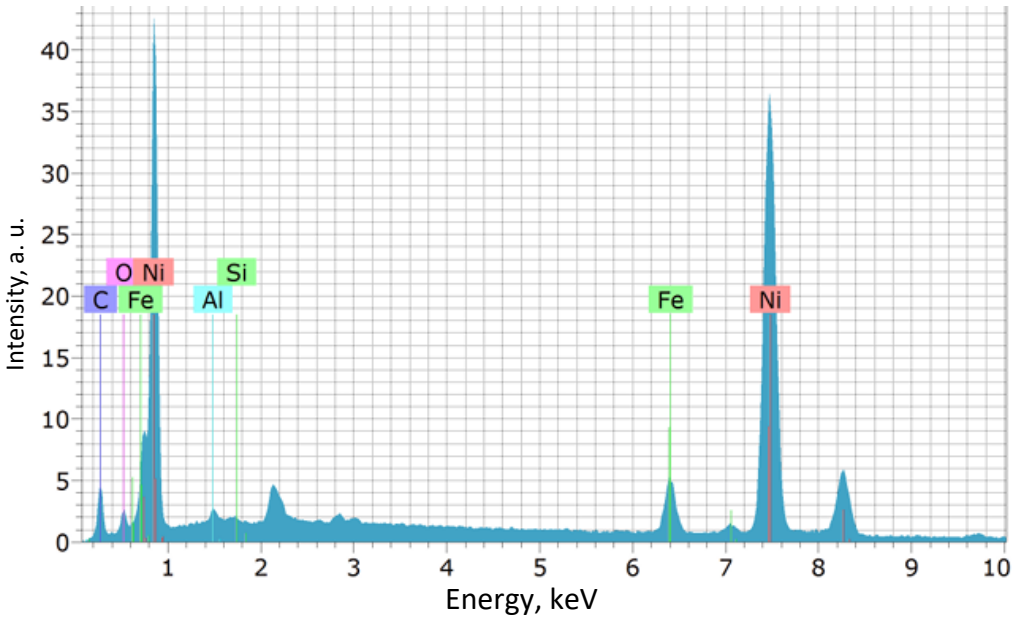


Figure 2. *EDS spectrum showing peaks of elements coated on tool*

The limited thickness of the Pd coating and the EDS electron beam's penetration depth allow X-rays from the underlying substrate to contribute considerably to the spectrum, resulting in a comparatively weak Pd signal relative to the Ni signal. The presence of a Pd-coated Ni-based metallic needle utilized in the electrochemical machining tests is thus confirmed by the EDS data.

The constituent composition and EDS spectra of the electrochemical machining needle electrode are displayed in Table 1. With a normalized concentration of 78.76 wt.% (49.10 at.%), the EDS analysis shows that nickel is the major element, indicating that the underlying needle substrate is Ni-rich. Iron is found at 4.75 wt.% (3.11 at.%), with trace amounts of silicon (0.05 wt.%) and aluminium (0.68 wt.%) as well. Oxygen is found at 1.58 wt.% (3.61 at.%), while carbon makes up 14.18 wt.% (43.19 at.%). Surface contamination, carbon tape, or the carbon coating/sample preparation used during EDS analysis could contribute to the comparatively high carbon content. The composition determined by the quantitative EDS analysis is compatible with the high Ni peaks seen in the spectrum, especially around 7.5 and 8.3 keV. Palladium was applied to the needle before it was used as the electrode, but

the quantitative EDS table does not show Pd as a significant constituent. This could be explained by the Pd coating's thinness relative to the incident electron beam's interaction volume, allowing the underlying Ni-rich substrate to control the EDS response. As a result, the current EDS examination does not, by itself, provide conclusive quantitative proof of the Pd coating; rather, it largely verifies the composition of the underlying needle substrate.

Experiments were conducted as shown in Table 2. Along with the $NaNO_3$ electrolyte, a concentration of 10 g L^{-1} of $C_6H_8O_6$ is used as a reducing agent to minimize sludge formation during the electrolysis process.

Table 1. *Elements on coated tool*

Element	Series	Unnormalized concentration, wt.%	Normalized concentration, wt.%	Concentration, at.%	Measurement error (3σ), wt.%
Carbon	K	12.16	14.18	43.19	6.43
Oxygen	K	1.35	1.58	3.61	1.00
Iron	K	4.08	4.75	3.11	0.44
Nickel	K	67.54	78.76	49.10	5.52
Aluminium	K	0.59	0.68	0.93	0.19
Silicon	K	0.04	0.05	0.06	0.09
Total		85.75	100.00	100.00	

Table 2. *Experimental factors in ECM of AISI 304 SS*

Exp. No	Electrolyte concentration, mol L^{-1}	Machine voltage, V	Duty cycle, %	Frequency, Hz	MR, µm s^{-1}	OC, µm
1	0.328	12	90	90	0.167	280
2	0.339	12	90	90	0.185	267
3	0.351	12	90	90	0.208	252
4	0.363	12	90	90	0.219	232
5	0.375	12	90	90	0.231	230
6	0.386	12	90	90	0.238	228
7	0.386	7	90	90	0.189	302
8	0.386	8	90	90	0.208	290
9	0.386	9	90	90	0.225	286
10	0.386	10	90	90	0.238	274
11	0.386	11	90	90	0.269	254
12	0.386	12	90	90	0.278	244
13	0.386	12	40	90	0.198	294
14	0.386	12	50	90	0.214	288
15	0.386	12	60	90	0.231	273
16	0.386	12	70	90	0.253	244
17	0.386	12	80	90	0.287	234
18	0.386	12	90	90	0.298	216
19	0.386	12	90	40	0.219	290
20	0.386	12	90	50	0.238	270
21	0.386	12	90	60	0.253	260
22	0.386	12	90	70	0.298	250
23	0.386	12	90	80	0.309	230
24	0.386	12	90	90	0.347	222

Results and discussion

Effect of electrolyte concentration on machining rate and overcut

Figure 3 shows how electrolyte concentration affects MR and OC during ECM of AISI 304 SS using a $NaNO_3$ electrolyte that contains 10 g L^{-1} ascorbic acid. The machining voltage, duty cycle, and pulse frequency were kept at 12 V, 90 % and 90 Hz, respectively, while the electrolyte content was

(cc) BY

adjusted between 0.328 and 0.386 mol L^{-1}. The figure clearly shows that the MR rose by around 42.5 %, from 0.167 µm s^{-1} at 0.328 mol L^{-1} to 0.238 µm s^{-1} at 0.386 mol L^{-1}. This enhancement is explained by the electrolyte conductivity increasing with concentration, which improves the IEG's ionic mobility and current density. By encouraging more effective anodic breakdown of the workpiece material, the increased current density raises the MR [20].

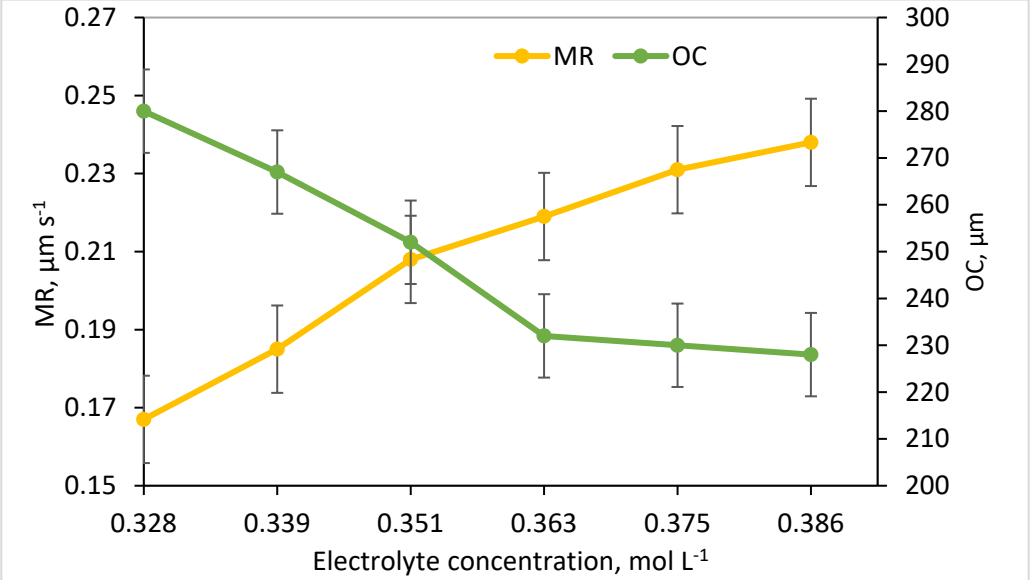


***Figure 3**. Plots of MR and OC* vs. *electrolyte concentration*

On the other hand, as the electrolyte content increased from 0.328 and 0.386 mol L^{-1}, the OC steadily dropped from 280 to 228 µm, indicating a decrease of almost 18.6 %. The reduction in overcut suggests better anodic dissolution localization because of more even current distribution and improved reaction product flushing. This effect was further enhanced by the addition of 10 $g.L^{-1}$ ascorbic acid, which functions as a reducing agent to prevent the production of insoluble iron hydroxide sludge. Ascorbic acid reduces passive film development and maintains steady electrolyte conductivity during the machining process by converting ferric ions (Fe^{3+}) to ferrous ions (Fe^{2+}) and keeping dissolved metal species in the electrolyte.

Overall, the findings show that by concurrently raising the MR and lowering the OC, raising the electrolyte concentration within the studied range greatly improves machining performance. Under the chosen experimental conditions, an electrolyte concentration of 0.386 mol L^{-1} provided the highest MR (0.238 µm s^{-1}) and the lowest OC (228 µm), indicating the best balance between dimensional accuracy and machining productivity. These results verify that electrolyte concentration is a crucial process parameter controlling the effectiveness and calibre of AISI 304 SS ECM.

The standard deviation of three repeated experimental trials carried out at each electrolyte concentration is shown by the error bars. The comparatively modest error bars show that the experimental measurements were highly precise and have strong reproducibility. Electrolyte concentration has a consistent, quantifiable impact on ECM performance, as shown by the steady increase in MR and corresponding decrease in OC, which are far greater than the experimental variability. Although the total experimental uncertainty is still minimal, the dependability of the acquired data is confirmed. The modest increase in variability found at intermediate electrolyte concentrations may be related to transient changes in electrolyte flow characteristics and gas bubble evolution.

Effect of machining voltage on machining rate and overcut

The impact of machining voltage on the MR and OC during ECM of AISI 304 stainless steel using a $NaNO_3$ electrolyte containing 10 g L^{-1} ascorbic acid is shown in Figure 4. The electrolyte concentration, duty cycle, and pulse frequency were kept constant at 0.386 mol L-1, 90 %, and 90 Hz, respectively, while the machining voltage was adjusted between 7 and 12 V. In particular, the MR increased by around 47.1 %, from 0.189 µm s^{-1} at 7 V to 0.278 µm s^{-1} at 12 V. This improvement is explained by the increased electric field intensity across the IEG, which, in accordance with Ohm's law, results in a larger current density. The MR is improved because the higher current density speeds up the anodic disintegration of AISI 304 SS. A discernible rise in MR between 10 V and 11 V indicates that there is enough electrical energy available to counteract polarization effects and promote quick electrochemical disintegration [21]. As the machining voltage increased from 7 V to 12 V, the OC simultaneously dropped from 302 to 244 µm, a reduction of almost 19.2 %. Higher OC and more lateral machining result from the comparatively low current density at lower voltages, which also encourages stray-current effects and non-uniform material dissolution. Dimensional accuracy improves as the voltage rises because the electrochemical reaction becomes more confined inside the machining zone.

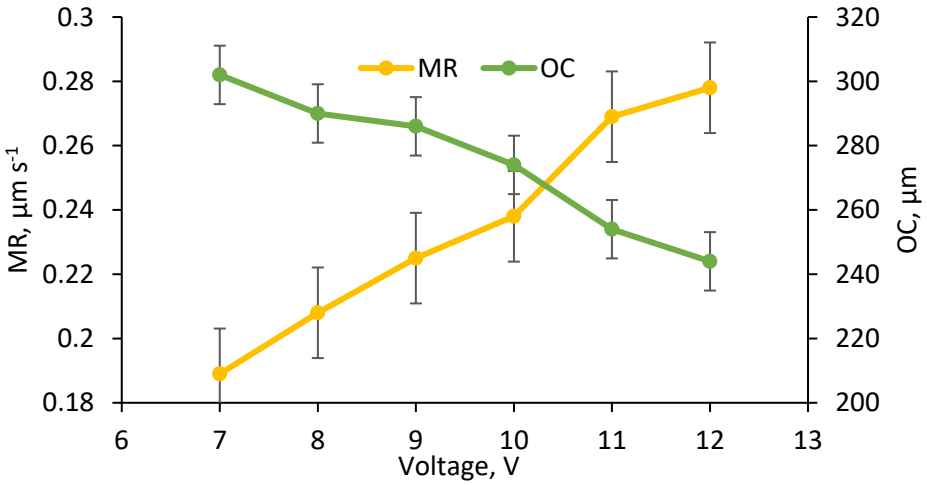


Figure 4. *Plots of MR and OC* vs. *machining voltage*

The decrease in OC also suggests that reaction products and gas bubbles are being removed from the IEG more effectively, preserving a stable machining environment. By converting ferric ions (Fe^{3+}) to ferrous ions (Fe^{2+}) and lowering the precipitation of insoluble iron hydroxides, the addition of 10 g L^{-1} ascorbic acid further improves machining stability. This results in more consistent anodic dissolution at higher machining voltages by suppressing sludge development, preserving electrolyte conductivity, and reducing passive film formation on the workpiece surface.

Overall, the findings show that machining voltage is an important factor affecting dimensional accuracy and machining productivity. Increasing the voltage enhanced electrochemical dissolution within the studied range, leading to a lower OC and a higher MR. With a maximum MR of 0.278 µm s^{-1} and a relatively low OC of 244 µm, the ideal machining voltage of 12 V demonstrated effective ECM under the chosen electrolyte conditions. These results confirm that higher machining voltages improve overall ECM performance and promote stable localized dissolution.

The standard deviation from three repeated experimental attempts at each voltage level is shown by the error bars. High experimental precision and outstanding repeatability of both machining rate and overcut measurements are indicated by the comparatively narrow error bars.

(cc) BY

The observed trends are statistically credible since the rise in machining rate and corresponding decrease in overcut with increasing voltage are significantly larger than the experimental variability. Although localized electrolyte turbulence, gas bubble formation, and small variations in current distribution may cause minor variations at intermediate voltage levels, the overall experimental uncertainty remains low, indicating the stability and repeatability of the ECM process.

Effect of duty cycle on machining rate and overcut

The impact of duty cycle on MR and OC during ECM of AISI 304 SS employing a $NaNO_3$ electrolyte containing 10 g L^{-1} ascorbic acid is shown in Figure 5. The electrolyte concentration, machining voltage, and pulse frequency were kept constant at 0.386 mol L^{-1}, 12 V, and 90 Hz, respectively, while the duty cycle was adjusted between 40 and 90 %. The graph shows that MR increased steadily with duty cycle. The MR improved by about 50.5 %, rising from 0.198 µm s^{-1} at 40 % duty cycle to 0.298 µm s^{-1} at 90 % duty cycle. The longer pulse-on time linked to higher duty cycles, which permits more charge transfer across the IEG during each machining cycle, is responsible for this increase [21].

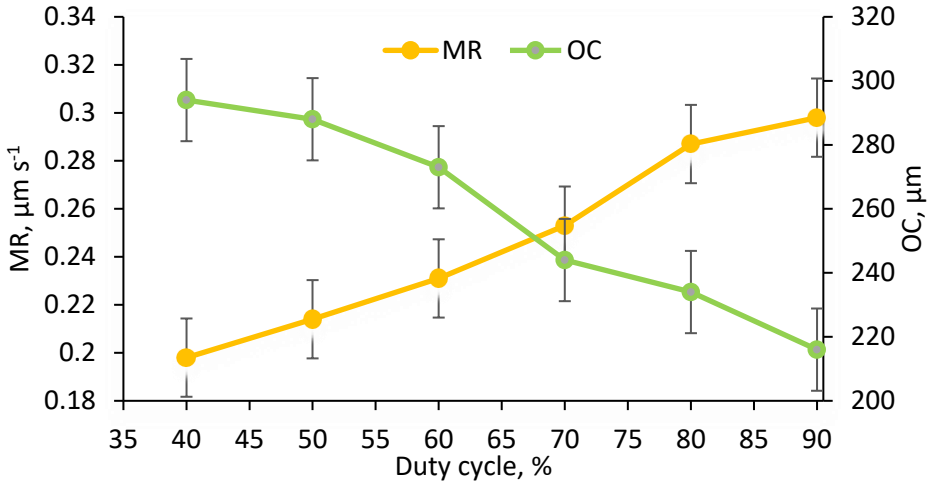


***Figure 5**. Plots of MR and OC* vs. *duty cycle*

Higher MR results from the anodic disintegration of AISI 304 SS becoming more efficient. Sufficient electrochemical energy is available for effective and stable metal dissolution while preserving adequate electrolyte replenishment during the pulse-off period, as shown by the steady increase in MR up to 70 % duty cycle and the more noticeable rise between 70 and 80 %. On the other hand, the OC dropped by around 26.5 %, from 294 µm at 40 % duty cycle to 216 µm at 90 % duty cycle. Increased lateral material removal and greater OC arise from the shorter pulse-on length at lower duty cycles, which restricts the electrochemical reaction and causes non-uniform anodic dissolution.

Dimensional precision improves as the duty cycle rises because the electrochemical disintergration becomes steadier and more confined. Additionally, the improved pulse-on time reduces stray current effects and minimizes OC by promoting uniform current distribution throughout the machining zone. By acting as a reducing agent and preventing the production of insoluble iron hydroxide sludge, the addition of 10 g. L^{-1} ascorbic acid to the $NaNO_3$ electrolyte further enhances machining performance. Ascorbic acid improves continuous anodic dissolution, reduces passive film generation on the workpiece surface, and preserves electrolyte clarity and conductivity by converting Fe^{3+} ions to Fe^{2+} ions. In addition to improving machining stability, this helps to simultaneously raise MR and lower OC. Error ranges between experimental replicates are represented by the error bars for all parameters. The observed trends for both MR and OC are statistically significant

($p < 0.05$) and not due to random error from experimental scatter, as confirmed by the distinct separation between data points at 40 and 90 %.

Overall, the findings show that one of the most important process variables influencing ECM performance is duty cycle. Increasing the duty cycle significantly increased dimensional accuracy and machining productivity within the examined range. The maximum MR of 0.298 µm s^{-1} and the lowest overcut of 216 µm were obtained with the ideal duty cycle of 90 %, demonstrating improved ECM performance. These results imply that a greater duty cycle offers the best compromise between accurate AISI machining, stable electrolyte flow, and effective anodic dissolution.

Effect of pulse frequency on machining rate and overcut

The impact of pulse frequency on MR and OC during ECM of AISI 304 SS using a $NaNO_3$ electrolyte containing 10 g L^{-1} ascorbic acid is shown in Figure 6. The electrolyte content, machining voltage, and duty cycle were kept constant at 0.386 mol L^{-1}, 12 V and 90 %, respectively, while the pulse frequency was adjusted between 40 and 90 Hz. The findings show that as pulse frequency increased, MR gradually increased. The MR improved by about 58.4 %, rising from 0.219 µm s^{-1} at 40 Hz to 0.347 µm s^{-1} at 90 Hz. The improved pulse characteristics at higher frequencies, which promote the localization of electrochemical dissolution and enable quick electrolyte regeneration within the IEG, are responsible for the rise in MR [22,23].

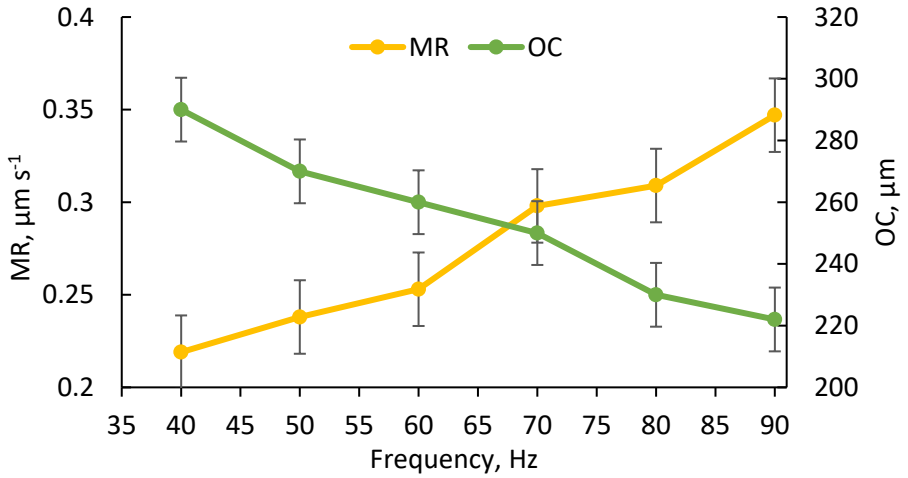


***Figure 6**. Plots of MR and OC* vs. *pulse frequency*

While ensuring a steady supply of fresh electrolyte to the machining zone, shorter pulse durations reduce concentration polarization. Higher pulse frequencies also facilitate the effective removal of dissolved reaction products and hydrogen bubbles, keeping the current density steady and speeding up anodic dissolution. Increased electrochemical efficiency is indicated by a discernible increase in MR between 60 and 70 Hz because of increased electrolyte cleansing and fewer diffusion limits. On the other hand, the OC steadily dropped from 290 µm at 40 Hz to 222 µm at 90 Hz, a decrease of almost 23.4%. The longer pulse duration at lower pulse frequencies prolongs the workpiece's exposure to the electric field, increasing the effects of stray current and lateral dissolution.

Dimensional precision improves as pulse frequency rises because the electrochemical reaction is more confined to the designated machining zone. The decrease in OC also results from better removal of gaseous products, dissolved metal ions, and machining debris from the inter-electrode gap, which reduces unwanted side-wall dissolution. By acting as a reducing agent and preventing the formation of insoluble iron hydroxide sludge, adding 10 g L^{-1} ascorbic acid to the $NaNO_3$ electrolyte further improves machining. Ascorbic acid maintains electrolyte conductivity throughout machining, prevents

(cc) BY

passive layer formation on the workpiece surface, and stabilizes the electrolyte by converting Fe^{3+} ions to Fe^{2+} ions [24,25]. As a result, even at higher pulse frequencies, the electrochemical dissolution is consistent, improving surface quality and machining efficiency. For both MR and OC, the error bar lengths are essentially the same at all frequency levels. This shows steady experimental repeatability and constant measurement accuracy over the frequency range. There is no overlap between the error boundaries when comparing 40 and 90 Hz directly. This demonstrates that an increase in MR is driven solely by higher frequency. A statistically substantial decrease in overcut is confirmed by the non-overlapping error bars between 40 Hz and 80 to 90 Hz.

Overall, the findings show that, out of all the variables examined, pulse frequency has the greatest impact on the machining rate. Increasing the pulse frequency improved dimensional accuracy and machining productivity by minimizing overcut and greatly increasing material removal. With a low overcut of 222 µm and the greatest machining rate of 0.347 µm s^{-1}, the optimal pulse frequency of 90 Hz demonstrated superior ECM performance under the chosen working circumstances. These results demonstrate that higher pulse frequencies enhance electrolyte renewal, stabilize current distribution, and encourage localized anodic dissolution, leading to accurate and effective AISI 304 SS machining.

The SEM micrographs (Figures 7 and 8) of the ECM AISI 304 SS specimen employing the $NaNO_3$ + + $C_6H_8O_6$ electrolyte show a clearly defined and nearly circular machined hole, indicating controlled anodic dissolution throughout the ECM process. The inclusion of ascorbic acid reduced localized current fluctuations and improved electrochemical stability, as shown by the consistent hole shape and comparatively smooth edges. There are very few tiny particle deposits around the edge of the hole. When compared to machining with $NaNO_3$ alone, the quantity of corrosion products and machining sludge is substantially reduced. This improvement is caused by the antioxidant and reducing agent ascorbic acid.

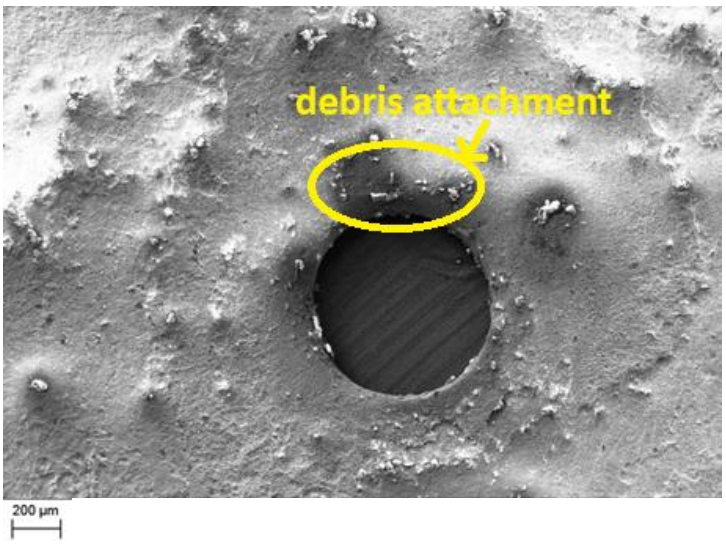


Figure 7. *SEM image of hole*

Ascorbic acid prevents the oxidation of dissolved metal ions, promotes their removal from the IEG, and reduces the formation of insoluble iron, chromium, and nickel hydroxides. Consequently, electrolyte circulation remains effective, leading to more reliable anodic dissolution. Reduced accumulation of reaction products reduces electrolyte blockage and stray-current distribution, improving dimensional accuracy and lowering OC. The smooth transition between the machined hole and the surrounding surface indicates that side-wall disintegration is effectively managed, resulting in a cleaner machined profile.

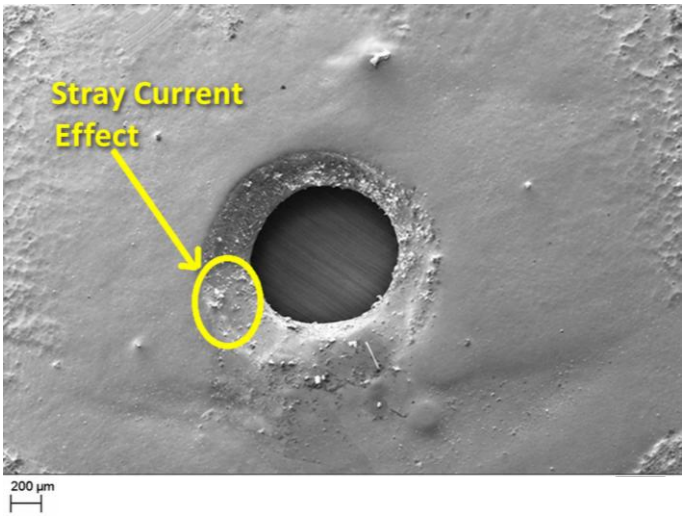


Figure 8. *SEM image of hole with stray current effect*

The surrounding surface shows no signs of serious side-wall disintegration or errant machining. The small overcut area around the hole suggests that the electrolyte may have maintained a constrained current distribution, improving dimensional accuracy. Furthermore, it reduces workpiece surface passivation, as shown by the cleaner machining zone. Overall, the SEM data show that adding ascorbic acid to the $NaNO_3$ electrolyte improves surface integrity, reduces sludge development, limits passive-layer deposition, and produces cleaner hole geometry, all of which improve ECM performance. The mixed electrolyte system promotes stable anodic dissolution, which enhances surface quality and machining accuracy. The findings of this study are compared with the existing literature, and it's found that the ascorbic acid mixed electrolyte produces the lowest OC of 216 µm compared with the literature value of 222 µm [26,27].

Conclusions

Under the chosen experimental conditions, the investigated palladium-coated electrode and ascorbic acid-modified $NaNO_3$ electrolyte configuration showed favourable machining characteristics. Ascorbic acid acted as a reducing agent by converting Fe^{3+} to Fe^{2+}, which prevented the formation of insoluble iron hydroxide sludge, decreased the formation of passive films, and maintained electrolyte conductivity throughout the machining process. These electrochemical effects promoted consistent anodic dissolution and increased machining efficiency. The experimental results showed that all four machining parameters electrolyte content, machining voltage, duty cycle, and pulse frequency had a substantial effect on MR and OC.

The needle electrode's Ni-rich composition (78.76 wt.% Ni) was confirmed by EDAX analysis, but trace amounts of Fe, Al and Si were also found. The lack of a discernible Pd signal indicates that the thin Pd coating was below the EDS analysis's effective detection depth, with the underlying Ni-based substrate mostly influencing the spectrum.

When the electrolyte content was increased from 23 to 28 g L^{-1}, the MR rose from 0.167 to 0.238 µm s^{-1} and the OC dropped from 280 to 228 µm. Similarly, increasing the machining voltage from 7 to 12 V increased the cutting rate to 0.278 µm s^{-1} and reduced the OC to 244 µm. Higher duty cycles raised the MR to 0.298 µm s^{-1} while reducing the OC to 216 µm, while raising the pulse frequency to 90 Hz produced the highest MR of 0.347 µm s^{-1} with an overcut of 222 µm.

These results show that improved electrical and pulse parameters concurrently increase machining productivity, localized anodic dissolution, and dimensional accuracy. SEM analysis further

(cc) BY

confirmed the beneficial role of ascorbic acid in the electrolyte. The drilled holes were almost round, had smooth edges, minimal sludge deposition, and minimal errant cutting. The absence of micro-spark-affected regions and microcracks verified that material removal occurred only through electrochemical dissolution while maintaining the metallurgical integrity of AISI 304 SS. The reduced accumulation of corrosion products and passive films demonstrated ascorbic acid's ability to maintain a clean IEG and ensure uniform current distribution.

Overall, comparative studies are needed to establish its performance advantages over conventional electrode-electrolyte systems.

Funding: *There is no funding for this research*

Conflict of interest*: The authors declare that they have no known competing financial interests or personal relationships that could have appeared to influence the work reported in this paper*

References

[1] H. M. Yehia, F. Nouh, O. A. El-Kady, W. Abd-Elaziem, E. M. Elsayed, Studying the microstructure, electrical, and electrochemical behaviour of the Cu-10WC/x GNs for electrochemical machining electrode and energy application, *International Journal of Machining and Machinability of Materials* **24** (2022) 430-452. https://doi.org/10.1504/IJMMM.2022.128461

[2] Q. C. Kong, G. L. Liu, J. L. Song, Q. F. Tan, G. Z. Liu, S. Q. Zhao, Preparation of sidewall-insulation layer on micro-hollow electrodes for ECM by asymmetric-timed bipolar electrophoretic coating method and its application, *Precision Engineering* **67** (2021) 24-35. https://doi.org/10.1016/j.precisioneng.2-020.09.001

[3] J.-C. Hung, Y.-R. Liu, H.-P. Tsui, Z.-W. Fan, Electrode insulation layer for electrochemical machining fabricated through hot-dip aluminizing and microarc oxidation on a stainless-steel substrate, *Surface and Coatings Technology* **378** (2019) 124995. https://doi.org/10.10-16/j.surfcoat.2019.124995

[4] J. Hung, H. Liu, Y. Chang, K. Hung, S. Liu, Development of helical electrode insulation layer for electrochemical microdrilling. *Procedia CIRP* **6** (2013) 373-377. https://doi.org/10.1016/j.procir.2013.03.045

[5] A. K. Swain, M. M. Sundaram, K. P. Rajurkar, Use of coated microtools in advanced manufacturing: An exploratory study in electrochemical machining (ECM) context, *Journal of Manufacturing Processes* **14** (2012), 150-159. https://doi.org/10.1016/j.jmapro.2011.11.005

[6] J.-C. Hung, P.-C. Chen, Characteristics research of different electrode tip shapes by electrodeposition for micro slot ECM, *Procedia CIRP* **95** (2020) 798-802. https://doi.org/10.1016/j.procir.2020.02.327

[7] G. H. Liu, Y. Li, X. P. Chen, S. J. Lv, Research on side-insulation of tool electrode for micro electrochemical machining, *Advanced Materials Research* **60** (2009) 380-387. https://doi.org/10.4028/www.scientific.net/AMR.60-61.380

[8] G. Liu, Y. Li, Q. Kong, H. Tong, H. Zhong, Silicon-based tool electrodes for micro electrochemical machining, *Precision Engineering* **52** (2018) 425-433. https://doi.org/10.1016/j.precisioneng.2018.02.003

[9] L. Guodong, L. Yong, K. Quancun, T. Hao, Selection and optimization of electrolyte for micro electrochemical machining on stainless steel 304, *Procedia CIRP* **42** (2016) 412-417. https://doi.org/10.1016/j.procir.2016.02.223

[10] M. Tak, S. V. Reddy A. Mishra, R. G. Mote, Investigation of pulsed electrochemical micro-drilling on titanium alloy in the presence of complexing agent in electrolyte, *Journal of Micromanufacturing* **1** (2018) 142-153. https://doi.org/10.1177/2516598418784682

[11] A. Sethi, B. R. Acharya, P. Saha, Electrochemical dissolution of WC-Co micro-tool in micro-WECM using an Eco-friendly citric acid mixed $NaNO_3$ electrolyte, *Journal of The Electrochemical Society* **169** (2022) 033503. https://doi.org/ 10.1149/1945-7111/ac54d9

[12] G. Cercal, G. de Alvarenga, M. Vidotti, Sludge reduction and surface investigation in electrochemical machining by complexing and reducing agents, *Processes* **11** (2023) 2186. https://doi.org/10.3390/pr11072186

[13] M. Zohoor, S. Jalili, A. Alipour, R. Mosallanejad, Effect of electrolyte type on electrochemical machining of 304 steel, *International Journal of Applied Engineering Research* **12** (2016) 20-39. https://www.ripublication.com/ijaer.htm

[14] D. Janardhanan, H. Perianna, Experimental investigation on the suitability of dual fluid system-assisted ECM (DF-ECM) and the influence of magnet in machining of SS304, *The International Journal of Advanced Manufacturing Technology* **130** (2024) 3819-3836. https://doi.org/10.1007/s00170-024-12957-6

[15] V. N. Najm, M. M. Abdulrazaq, A. M. S. Ahmed, Enhancing surface integrity of 316 SS with ecofriendly electrolyte in electrochemical machining, *Advances in Science and Technology. Research Journal* **19** (2025) 109-119. https://doi.org/10.12913/22998624/210085

[16] N. K. Jain, V. K. Jain, Optimization of electro-chemical machining process parameters using genetic algorithms, *Machining Science and Technology* **11** (2007) 235-258. https://doi.org/10.1080/10910340701350108

[17] R. Mishra, R. P. Singh, R. K. Garg, Investigation into micro slotting of Cu-based shape memory alloy via μ-ECM using ethylene glycol mixed aqueous NaCl electrolyte, *Canadian Metallurgical Quarterly* **64** (2025) 1063-1077. https://doi.org/10.1080/00084433.2024.2419224

[18] S. Wang, W. Wei, Y. Gao, H. Pan, Y. Wang, Characterization of Ti–Zr–V thin films deposited by DC and unipolar pulsed DC magnetron sputtering, *Vacuum* **188** (2021) 110200. https://doi.org/10.1016/j.vacuum.2021.110200

[19] Y. Ni, W. Wang, C. Tang, J. Sun, W. Zhang, W. Gao, J. Zou, Optimizing coverage of palladium nanoparticles for a highly sensitive hydrogen gas sensor based on nanogaps via spray-deposition, *Journal of Materials Science: Materials in Electronics* **35** (2024) 770. https://doi.org/10.1007/s10854-024-12537-0

[20] N. Sivashankar, K. Santhanam, S. Prasad, M. Jawahar, R. Thanigaivelan, Electrochemical micromachining of galvanized iron sheets: process optimization and performance evaluation, *Journal of Electrochemical Science and Engineering* **15** (2025) 2821. https://doi.org/10.5599/jese.2821

[21] V. Palaniswamy, T. Rajasekaran, Performance of magnetized tool in electrochemical micromachining on scrapped alloy wheel matrix composite, *Journal of Electrochemical Science and Engineering* **13** (2023) 553-561. https://doi.org/10.5599/jese.1660

[22] R. Health Royal Hermonson, R.Thanigaivelan, V. Kavya, K. Rathinasamy, T. Jagadeesha, Performance of electrochemically deposited hydroxyapatite on textured 316L SS for applications in biomedicine, *Surface Engineering* **39** (2023) 882-891. https://doi.org/10.1080/02670844.2023.2265616

[23] V. Palaniswamy, K. Seeniappan, T. Rajasekaran, N. Lakshmaiya, Enhancing MRR and accuracy with magnetized graphite tool in electrochemical micromachining of copper: original scientific paper, *Chemical Industry & Chemical Engineering Quarterly* **29** (2023) 201-208. https://doi.org/10.2298/CICEQ220731027P

[24] R. Thanigaivelan, R. M. Arunachalam, C. Madhan, R. R. Kumar, M. Muthuselvam, Impact of electrochemical passivation on Burr suppression of Ti–4Al–6V alloy during machining, *Surface Engineering and Applied Electrochemistry* **55** (2019) 424-429. https://doi.org/10.3103/S106837551904015X

(cc) BY

[25] N. Sivashankar, R. Thanigaivelan, L. Selvarajan, K. Venkataramanan, Investigation of electrochemical micromachining on magnesium alloy using hollow tool electrode, *Ultrasonics* **147** (2025) 107526. https://doi.org/10.1016/j.ultras.2024.107526
[26] R. Thanigaivelan, N. Rajan, M. Soundarrajan, R. Priya, Influence of mixed electrolyte in electrochemical micromachining on SS316L, *Manufacturing Technology Today* **20(7-8)** (2021) 16-25. https://mtt.cmti.res.in/index.php/journal/article/view/9
[27] S. Maniraj, R. Thanigaivelan, Effect of electrode heating on performance of electrochemical micromachining, *Materials and Manufacturing Processes* **34** (2019) 1494-1501. https://doi.org/10.1080/10426914.2019.1655153

©2026 by the authors; licensee IAPC, Zagreb, Croatia. This article is an open-access article distributed under the terms and conditions of the Creative Commons Attribution license (http://creativecommons.org/licenses/by/4.0/)